Biomolecule Detection

DOI: 10.1002/anie.200903472

Multiplex Label-Free Detection of Biomolecules with an Imprinted Suspension Array**

Yuan-Jin Zhao, Xiang-Wei Zhao, Jing Hu, Juan Li, Wen-Yu Xu, and Zhong-Ze Gu**

Multiplex detection of biomolecules has facilitated clinical diagnosis, drug discovery, and environmental testing.[1–4] Immunoassays using labeled antibodies are the most popular methods for the detection of biomolecules because of their sensitivity and selectivity. However, labeling protocols are time-consuming and expensive, and may alter the form or physicochemical behavior of the antibodies, which could lead to false negative results.[5–7] In addition, the reagent stability, high cost, and difficulties associated with antibody production, together with the adverse action of toxic compounds or immunosuppressants on the metabolism and the immune system during the production of antibodies, are often cited as problems.[7] Therefore, it is highly desirable to carry out multiplex label-free detection of biomolecules without using immunoassay methods.

Suspension arrays, which use self-encoded microcarriers as elements,[8–14] have shown obvious advantages in the multiplex detection of biomolecules. However, few of them can be used for the label-free detection of biomolecules.[15,16] Moreover, these methods are still based on the use of probe antibodies. In contrast, molecularly imprinted polymers (MIPs) have unique properties as mimics of natural molecular receptors that may make them suitable for revolutionary applications in biotechnology.[17–19] Recently, many kinds of MIP sensors have been developed for the detection of biomolecules based on physicochemical responses of the MIPs, such as changes in refractive index and volume.[20,21] However, these sensors could respond only to single analytes, and the detection signals from the physicochemical response of the MIPs were not distinct and were difficult to measure with accuracy.

Herein, we report a new type of suspension array for the multiplex label-free detection of biomolecules without using immunoassay methods. The microcarriers of our suspension array are molecularly imprinted polymer beads (MIPBs) with photonic crystal structure, which not only provide diffraction peaks for encoding but also convert the slight physicochemical response signals to the obvious changes of optical signals.[22–24] This technique combines the advantages of suspension arrays, molecular imprinting, and photonic crystal sensors.

As a proof of concept for the multiplex label-free detection of biomolecules not based on immunoassay methods, we constructed an imprinted suspension array with affinity for proteins. For large biomacromolecules, surface imprinting was used for the fabrication of the MIPBs with photonic crystal structure due to the easy removal and rapid rebinding characteristics during assays. Scheme 1 outlines the preparation of the MIPBs by template replication. The protein template was first immobilized onto the surface of the nanoparticles in the prepared silica colloidal crystal beads (SCCBs).[16] Then an acrylamide solution was infused and polymerized in the voids of the SCCBs. Removal of the silica nanoparticles and the protein templates yielded polyacrylamide inverse opaline photonic crystal structure MIPBs with precisely positioned amide groups and "footprints" of the imprinted biomolecules on the surface of the macropores. The MIPBs display uniform color (Figure 1) and hexagonal symmetry surface structure (Figure 2). The macropores of the beads are interconnected and extend to the inside of the inverse opaline building-block MIPBs. They not only provide greater surface area and more interaction sites, but also offer easier access for the analytes to the recognition sites.

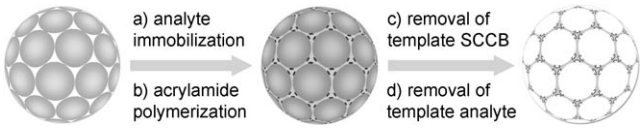

Scheme 1. Schematic diagram of the preparation method for molecularly imprinted polymer beads with photonic crystal structure.

For label-free detection, bovine hemoglobin (Hb) imprinted MIPBs were incubated in analyte solutions of various concentrations. When a biomolecule enters a complementary nanocavity, a multitude of simultaneous hydrogen bonds can be formed between the oriented amide groups in the nanocavity and the polar surface residues of the biomolecule. These cooperative, multivalent hydrogen bonds lead to a significantly increased selective biomolecule-binding affin-

[*] Y.-J. Zhao, Prof. X.-W. Zhao, J. Hu, J. Li, W.-Y. Xu, Prof. Z.-Z. Gu
State Key Laboratory of Bioelectronics
School of Biological Science and Medical Engineering
Southeast University, Nanjing 210096 (China)
Fax: (+86) 25-8379-5635
E-mail: gu@seu.edu.cn
xwzhao@seu.edu.cn
Prof. Z.-Z. Gu
Laboratory of Environment and Biosafety
Research Institute of Southeast University in Suzhou
Dushu Lake Higher Education Town, Suzhou 215123 (China)

[**] This research was supported by the 333 Talent Project Foundation of Jiangsu Province, Ministry of Science and Technology (grant no. 2006AA03Z331), the National Science Foundation of China (grant nos. 20703010), and the Jiangsu Natural Science Foundation (grant no. BK2008318).

Supporting information for this article is available on the WWW under http://dx.doi.org/10.1002/anie.200903472.

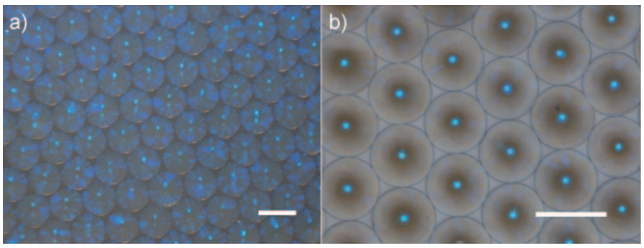

Figure 1. Three-dimensional image (a) and bright-field microscopic image (b) of the MIPBs in buffer solution. Scale bars: 300 μm.

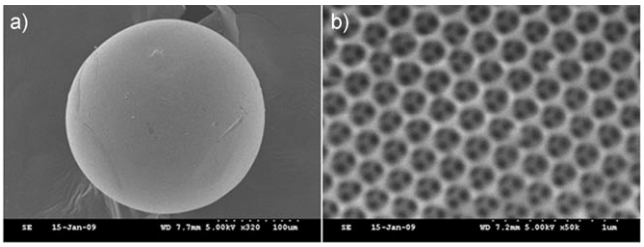

Figure 2. SEM images of an MIPB: a) low-magnification image of a bead. b) High-magnification image of the bead surface.

ity. The MIPBs reported this molecular recognition event through a gradual shift of the position of the Bragg diffraction peak to long wavelengths with an increase of the bovine Hb concentration (Figure 3). Remarkably, a trace amount of bovine Hb (1 ng mL^{-1}) was enough to lead to a red-shift of the diffraction peak. This phenomenon can be explained by Bragg's law under normal incidence [Eq. (1)],

$$\lambda = 1.633\, d\, n_{\text{average}} \quad (1)$$

where λ is the peak wavelength of the MIPBs, d is the distance between the centers of two neighboring nanopores, and n_{average} is the average refractive index of the MIPBs. During the process of molecular recognition, the bovine Hb binds to the water-filled nanocavities of the imprinted MIPs. As the refractive index of the protein is larger than that of water ($n_{\text{protein}} = 1.42$, $n_{\text{water}} = 1.33$), the n_{average} increases and thus the Bragg diffraction peak shifts to red. However, we observed a shift maximum of 13.5 nm in our experiment while the maximum shift caused by the change of n_{average} is less than 4 nm in theory (constant MIP volume and a 5 nm thickness of the bovine Hb layer on the nanopores of the MIPBs were assumed). Thus, the additional shift should be attributed to the increase of d, which is caused by swelling of the MIPs. To summarize, the specific binding of biomolecules on the imprinted nanocavities of the MIPBs leads to an increase in the average refractive index and the swelling of the MIPs, both of which are reported by the MIPBs through a red-shift of the Bragg diffraction peak.

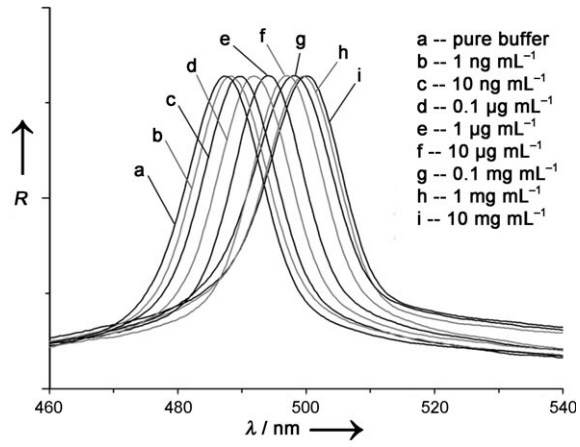

Figure 3. Optical response of the bovine Hb imprinted MIPBs incubated in solutions of bovine Hb at different concentrations.

To investigate the specificity of this method, Hb-imprinted MIPBs were tested with solutions of bovine serum albumin (BSA) and horseradish peroxidase (HRP). Figure 4a displays the optical response of the MIPBs in solutions of bovine Hb, BSA, and HRP. It can be observed that the MIPBs specifically recognize the template biomolecule (bovine Hb) and display negligible response to the control proteins. To further investigate the specificity of the MIPBs in protein recognition, human Hb, which has a similar amino acid sequence (differing in only 15% of the 574 amino acid positions) and three-dimensional structure to bovine Hb,[19] was introduced into the experiment. The results show that both the bovine Hb and human Hb imprinted MIPBs were able to discriminate between the two homologous proteins (Figure 4b). When the MIPBs were in binary mixtures of the biomolecules, they also exhibited high

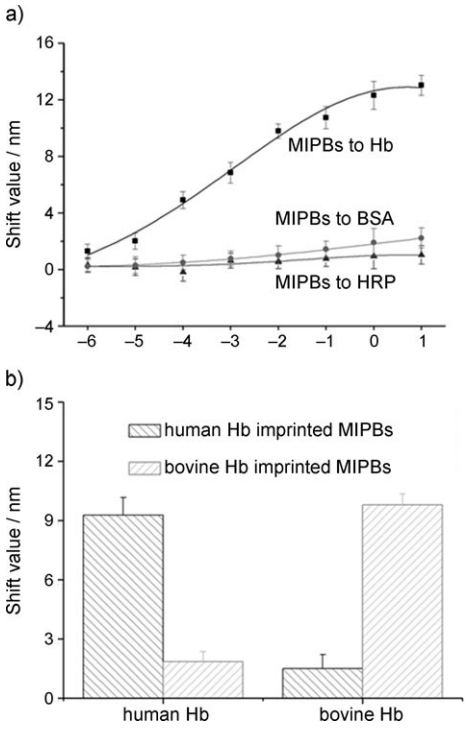

Figure 4. a) Plot of the Bragg shifts for the bovine Hb imprinted MIPBs in response to solutions of bovine Hb, BSA, and HRP at different concentrations. b) Bar diagram of the Bragg diffraction peak shifts of the two kinds of Hb-imprinted MIPBs incubated in either bovine Hb or human Hb (10 μg mL^{-1}). The number of replicates at any concentration was 5.

specificity (Figure S1 in Supporting Information). The comparative experiments proved that the MIPBs could be kept in PBS solution at 4 °C for at least one week without loss of affinity to their corresponding biomolecules.

To demonstrate the multiplexing capabilities of the imprinted suspension array for the label-free detection of biomolecules, we prepared three kinds of MIPBs imprinted with bovine Hb, HRP, and BSA by using 232 nm, 260 nm, and 285 nm nanoparticle composed SCCBs, respectively, as templates. The MIPBs were then mixed together and incubated in an analyte solution containing bovine Hb and HRP. Figure 5 shows the change of the diffraction peaks of the suspension array after multiplex assays. We observed that the diffraction peak of bovine Hb and HRP imprinted MIPBs shifts to longer wavelengths, while no detectable peak shift occurs on the BSA imprinted MIPBs. These results are consistent with the content of sample to which the imprinted MIPBs were exposed. As the diffraction peak shift of the MIPBs is less

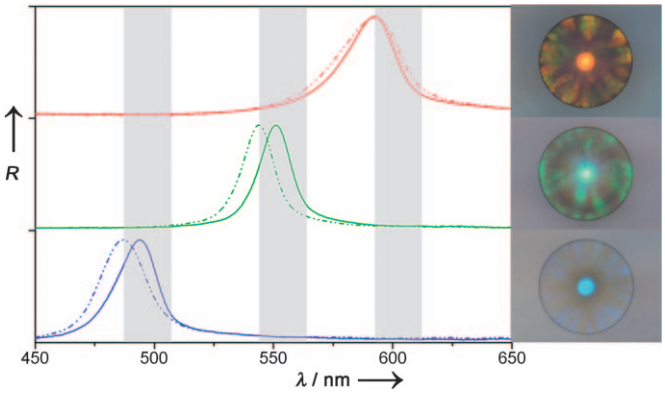

Figure 5. Reflection spectra (left) and bright field microscopic images (right) of three kinds of MIPBs. The cyan, green and red MIPBs were imprinted with bovine Hb, HRP, and BSA, respectively. The dashed lines and solid lines are the spectra of the MIPBs before and after multiplex detection. The gray areas are the encoding (spectral ranges from their initial diffraction-peak position to long wavelength 20 nm) of the MIPBs.

than 15 nm in our experiments, we can encode the MIPBs by the spectral ranges between the initial position of the diffraction peak to wavelengths 20 nm. longer. After protein binding and measurement of the diffraction peaks, the biomolecules were decoded by analyzing the spectral ranges of the diffraction peaks, and the amount of the bound biomolecules was estimated by the values of the diffraction peak shift. A powerful feature of this method is that both the decoding and biomolecule detection are as simple as a one-step measurement of the diffraction peak of the MIPBs, which simplifies the detection instruments and procedures. Theoretically, more than 30 kinds of molecules, which are generally enough for the demand of clinical diagnoses, can be detected simultaneously in the spectral range from 380 nm to 1000 nm by our suspension array without code interference. More encoding carriers can be fabricated by extending the spectral range or by introducing fluorescent dyes or quantum dots into the MIPBs.

In conclusion, we have introduced the molecular imprinting technique to suspension arrays and have realized the multiplex label-free detection of biomolecules without using immunological antibodies. The encoding carriers of our suspension array were MIPBs with photonic crystal structure. When used in multiplex label-free bioassays, they couple a readable shift in the diffraction peak to the binding events between the imprinted biomolecules and themselves, which can then be used for directly detecting and decoding multiple biomolecules simultaneously. The detection results reflect the sensitivity and specificity of the MIPBs. Therefore, this new type of suspension array is very promising in overcoming many restrictions of current techniques and is anticipated to open new horizons in medical diagnostics.

Received: June 26, 2009
Published online: September 3, 2009

Keywords: imprinting · photonic crystals · polymers · sensors · supramolecular chemistry

[1] D. R. Walt, *Science* **2000**, *287*, 451.
[2] D. P. Tang, R. Yuan, Y. Q. Chai, *Clin. Chem.* **2007**, *53*, 1323.
[3] F. Fleischhaker, A. C. Arsenault, F. C. Peiris, V. Kitaev, I. Manners, R. Zentel, G. A. Ozin, *Adv. Mater.* **2006**, *18*, 2387.
[4] F. Deiss, C. N. LaFratta, M. Symer, T. M. Blicharz, N. Sojic, D. R. Walt, *J. Am. Chem. Soc.* **2009**, *131*, 6088.
[5] M. Kyo, K. Usui-Aoki, H. Koga, *Anal. Chem.* **2005**, *77*, 7115.
[6] M. P. Schwartz, S. D. Alvarez, M. J. Sailor, *Anal. Chem.* **2007**, *79*, 327.
[7] J. L. Urraca, M. C. Moreno-Bondi, G. Orellana, B. Sellergren, A. J. Hall, *Anal. Chem.* **2007**, *79*, 4915.
[8] S. R. Nicewarner-Pena, R. G. Freeman, B. D. Reiss, L. He, D. J. Pena, I. D. Walton, R. Cromer, C. D. Keating, M. J. Natan, *Science* **2001**, *294*, 137.
[9] M. Han, X. Gao, J. Z. Su, S. Nie, *Nat. Biotechnol.* **2001**, *19*, 631.
[10] D. Y. Wang, A. L. Rogach, F. Caruso, *Nano Lett.* **2002**, *2*, 857.
[11] F. Cunin, T. A. Schmedake, J. R. Link, Y. Y. Li, J. Koh, S. N. Bhatla, M. J. Sailor, *Nat. Mater.* **2002**, *1*, 39.
[12] K. Braeckmans, S. de Smedt, C. Roelant, M. Leblans, R. Pauwels, J. Demeester, *Nat. Mater.* **2003**, *2*, 169.
[13] D. C. Pregibon, M. Toner, P. S. Doyle, *Science* **2007**, *315*, 1393.
[14] Y. J. Zhao, X. W. Zhao, C. Sun, J. Li, R. Zhu, Z. Z. Gu, *Anal. Chem.* **2008**, *80*, 1598.
[15] K. F. Kastl, C. R. Lowe, C. E. Norman, *Anal. Chem.* **2008**, *80*, 7862.
[16] Y. J. Zhao, X. W. Zhao, J. Hu, M. Xu, W. J. Zhao, L. G. Sun, C. Zhu, H. Xu, Z. Z. Gu, *Adv. Mater.* **2009**, *21*, 569.
[17] H. Shi, W. B. Tsai, D. M. Garrison, S. Ferrari, D. B. Ratner, *Nature* **1999**, *398*, 593.
[18] Y. Ge, A. P. F. Turner, *Trends Biotechnol.* **2008**, *26*, 218.
[19] Y. Li, H. H. Yang, Q. H. You, Z. X. Zhuang, X. R. Wang, *Anal. Chem.* **2006**, *78*, 317.
[20] X. B. Hu, G. T. Li, J. Huang, D. Zhang, Y. Qiu, *Adv. Mater.* **2007**, *19*, 4327.
[21] T. Miyata, M. Jige, T. Nakaminami, T. Uragami, *Proc. Natl. Acad. Sci. USA* **2006**, *103*, 1190.
[22] J. H. Holtz, S. A. Asher, *Nature* **1997**, *389*, 829.
[23] B. H. King, A. M. Ruminski, J. L. Snyder, M. J. Sailor, *Adv. Mater.* **2007**, *19*, 4530.
[24] M. M. Orosco, C. Pacholski, M. J. Sailor, *Nat. Nanotechnol.* **2009**, *4*, 255.

